THE JOURNAL OF PHYSICAL CHEMISTRY C

ARTICLE

pubs.acs.org/JPCC

Calcium-Based Functionalization of Carbon Materials for CO_2 Capture: A First-Principles Computational Study

C. Cazorla,[†,‡,§] S. A. Shevlin,[‡,§] and Z. X. Guo*[,‡,§]

[†]Institut de Ciència de Materials de Barcelona, 08193 Bellaterra, Spain

[‡]Department of Chemistry, University College London, London WC1H 0AH, United Kingdom

[§]London Centre for the Theory and Simulation of Materials, London WC1E 6BT, United Kingdom

ABSTRACT: We report a first-principles study of a CO_2 gas-sorbent material consisting of calcium atoms and carbon-based nanostructures. In the low gas pressure regime, we find that Ca decoration of nanotubes and graphene possess unusually large CO_2 uptake capacities (∼0.4−0.6 g CO_2/g sorbent) as a result of their topology and a strong interaction between the metal dopants and CO_2 molecules. Decomposition of the gas-loaded nanomaterials into CO gas and calcium oxide (CaO) is shown to be thermodynamically favorable; thus performance of the carbon capture process is further enhanced via formation of calcium carbonate ($CaCO_3$). Gas adsorption CO_2/N_2 selectivity issues have been also addressed with the finding that N_2 molecules bind to the metal-doped surfaces more weakly than CO_2 molecules. The predicted molecular binding and accompanying gas selectivity features strongly suggest the potential of Ca-doped carbon materials for CO_2 capture applications.

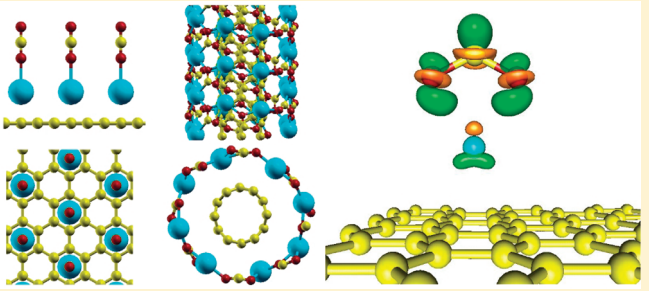

I. INTRODUCTION

The concentration of carbon dioxide (CO_2) in the atmosphere has increased by about 30% in the last 50 years, and it is likely to double over the next few decades as a consequence of anthropogenic fossil-fuel burning for energy generation.[1] Such an excess of CO_2 greenhouse gas may have dramatic negative repercussions on Earth's air quality and climate. Besides application of ecologically friendly energy policies, gas sequestration implemented in fossil-fuel energy plants and ambient air have been envisaged as promising and cost-effective routes to mitigate CO_2 accumulation in our atmosphere.[2−4] Present CO_2 capture and sequestration (CCS) strategies administered in fossil-fuel power generation plants mostly rely on scrubbing of flue gases (e.g., mixture of N_2, H_2O, CO_2 and SO_x gases that results from coal combustion) with liquid amine/ammonia solvents. Unfortunately, amine/ammonia solvent-based CCS technologies generally turn out to be not cost-effective due to the high energy penalty involved in solvent regeneration.[5] Currently, membranes and solid sorbents (e.g., activated carbons, zeolites, hydrotalcites and metal−organic frameworks) are widely considered as the pillars of next-generation CCS technologies because they present high gas-uptake capacities, great selectivity properties, and robust stability over repeated adsorption−desorption cycles.[6]

Activated carbons (AC), also known as activated charcoal or activated coal, are a form of carbon that has been processed in order to develop extreme porosity and large surface area; this family of carbons is widely used in industrial processes, and the costs associated to their production are low. In addition, ACs are easy to regenerate and insensitive to moisture. For all these reasons, carbon materials are among the most promising CO_2 sorbent candidates for mass generation.[6−8] Nevertheless, carbon-uptake capacities of AC under ambient conditions have been found to be lower than those of other materials like zeolites and molecular sieves.[9,10] Consequently, efforts based on chemical modification have been undertaken to enhance the CO_2 reactivity properties of AC. Examples include carbon functionalization with amines and amino groups,[11−13] impregnation with nitrogen-rich precursors,[14] and heat treatment in the presence of ammonia gas.[15] Despite the remarkable progress achieved with these techniques, present production expenses of chemically modified AC remain high due to the high temperatures and chemical substances involved in the treatments. Improvement of existing and prediction of new functionalization techniques, therefore, are crucial to accelerate the time required for deployment of economic AC-based CCS.

Surprisingly, detailed investigations on the interactions of CO_2 molecules with functionalized AC structures are very scarce. Consequently, the microscopic mechanisms underlying AC-mediated CCS are poorly understood at present. In this work, we are mainly concerned with advancing knowledge in this direction, and to this end we use first-principles quantum approaches. In particular, we explore a strategy for enhancement of the CO_2-reactivity properties of carbon materials which consists of surface doping with calcium atoms. The simulation approach that we employ is highly accurate, allowing access to

Received: February 23, 2011
Revised: April 26, 2011
Published: May 13, 2011

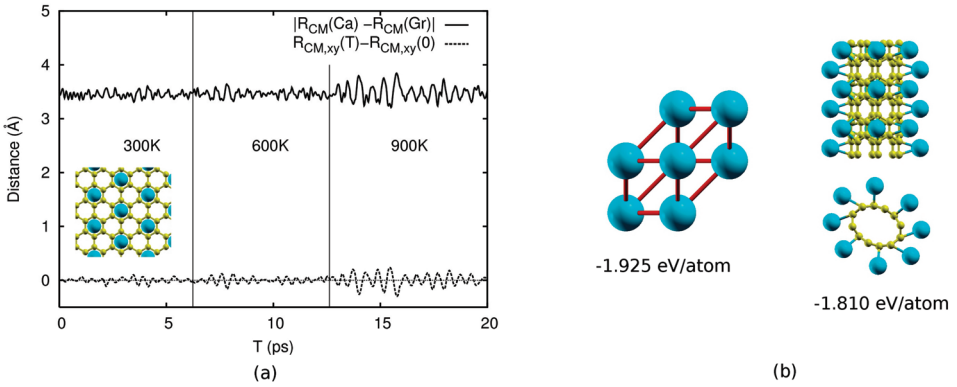

Figure 1. (a) Ab initio molecular dynamics results obtained at temperatures $300 \leq T \leq 900$ K: the trajectory of the center of mass (CM) of the Ca coating in the $(\sqrt{3} \times \sqrt{3})$ $R30$ °CaC_6 structure (inset) and its projection onto the graphene plane (arbitrarily defined as *xy*) as a function of time, are plotted relative to the center of mass of graphene (Gr) and starting optimized configuration, respectively. At high temperatures and for long simulation times, Ca atomic diffusion is not observed; thus room temperature stability of Ca-decorated graphene is demonstrated.[23] (b) Top and front views of the minimum energy structure determinated for Ca-decorated zigzag (6,0) CNT (right). The binding energy per Ca atom corresponding to this nanostructure ($X_{Ca} \approx 30\%$) is about 0.1 eV larger than the cohesive energy of bulk body-centered cubic Ca at equilibrium (left). Despite such an energy difference, formation of Ca clusters on the CNT surface is prevented by the presence of kinetic effects and the fact that typical Ca cluster cohesive energies are ∼0.5 eV/atom smaller than the cohesive energy of bulk solid Ca.[23] Ca and C atoms are represented as blue and yellow spheres, respectively.

Table I. Binding Energy per CO_2 Molecule and Corresponding Gas-Adsorption Capacities of Ca-Decorated Graphene and CNTs as a Function of Ca Concentration X_{Ca}[a]

	graphene		CNT (10,0) R = 3.96 Å		CNT (6,0) R = 2.42 Å	
X_{Ca} %	E_{bind}	CO_2 uptake	E_{bind}	CO_2 uptake	E_{bind}	CO_2 uptake
0.0	−0.035	0.153	−0.022	0.030	−0.010	0.153
$0.0 < X_{Ca} \leq 5.0$	−1.022	0.134	−1.865	0.085	−1.235	0.134
$5.0 < X_{Ca} \leq 15.0$	−2.731	0.323	−1.902	0.275	−1.543	0.239
$15.0 < X_{Ca} \leq 20.0$	−0.101	0.392	−2.283	0.440	−1.646	0.392
$20.0 < X_{Ca} \leq 30.0$			−2.846	0.549	−2.498	0.578

[a] First-row results were obtained for pristine nanostructures and last-row results for equilibrium Ca-decorated nanostructure geometries. Binding energies and carbon-uptake capacities are expressed in units of eV/molecule and g CO_2/g sorbent, respectively.

the electronic structure of the materials under study, thus the associated computational workload is very high; this implies that the number of atoms we can deal with in our calculations is reduced (∼100−200 atoms). For this reason, we have not attempted to simulate realistic AC structures, which are plagued with defects and thus require a prohibitively large number of atoms to be modeled accurately, but instead regular and computationally affordable carbon nanostructures (e.g., graphene and nanotubes). In other words, relevant AC features like porosity and surface texture have been overlooked at the expense of providing an accurate description of the atomic CO_2-sorbent interactions. It is worth noting, however, that since surface curvature effects are fully included in our calculations (we cover both flat graphene and cylindrical nanotubes) the general conclusions we arrive at can be reasonably extended to AC.

Gas adsorption capacities of pristine carbon nanotube (CNT) bundles have already been measured in experiments and analyzed with theory.[16−19] It has been shown that the interactions of CO_2 molecules with CNTs are of physisorption type[16−18] and that CNT CO_2 uptake capacities are remarkably twice that of activated carbon.[19] Recently, decoration of CNT-based membranes with Fe atoms has been proposed as a feasible technique for gas separation in flue gases.[20] Nevertheless, decoration of carbon nanostructures with transition metal atoms entails a series of important technical drawbacks, for instance a strong tendency for metal atom clustering, that in practice have impeded the realization of novel gas storage applications.[21,22] In a recent work, we have demonstrated that uniformly calcium-decorated graphene and zigzag CNTs become thermodynamically stable at moderately large doping concentrations[23] thus inherent coating difficulties posed by transition metals can be overcome by using alkali-earth metal species. Here, we assess the CCS potential of Ca-decorated nanostructures using ab initio computational approaches and find that these materials possess great CO_2 uptake capacities as a consequence of their topology and the attractive forces between gas molecules and Ca dopants. By great CO_2 uptake capacities we mean larger than the stipulated threshold value of 0.132 g CO_2/g sorbent for gas pressures lying within the range $0.1 \leq P \leq 1.0$ bar.[24] Moreover, formation of calcium oxide (CaO) and carbon monoxide (CO) in the CO_2-loaded nanostructures is found to be thermodynamically favorable. Such a tendency for calcium oxidation leads to a further enhancement in CCS performance via a secondary process in which calcium carbonate ($CaCO_3$) is generated.

II. THEORETICAL METHODS

Our calculations are based on the all-electron projector augmented wave implementation of density functional theory (DFT)[25] and the Perdew−Burke−Ernzerhof generalized gradient approximation (PBE-GGA) for the exchange-correlation energy,[26] as provided in the VASP code.[27] This method has been demonstrated to describe interactions between light molecules (e.g., H_2 and glycine) and metal centers as accurately as the Møller−Plesset second-order perturbation theory and coupled cluster approaches,[28,29] so that we assumed its validity for the present study. Electronic orbitals 2s2p, 3p4s, and 2s4p were considered in valence for C, Ca, and O atoms, respectively. A cutoff energy of 400 eV and dense *k*-point meshes, depending on

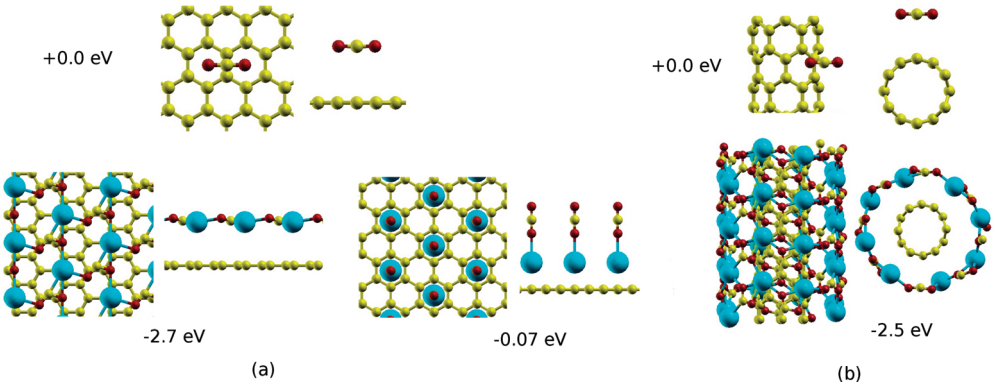

Figure 2. (a) Carbon capture geometry optimized structures obtained for pristine graphene (top) and Ca-doped graphene at 12.5% (bottom left) and 16.67% (bottom right) concentrations. (b) Carbon capture geometry optimized structures obtained for pristine (top) and 30% Ca-decorated (bottom) zigzag (6,0) CNT. Numbers in the figure correspond to the calculated binding energies relative to the nondoped cases. Ca, C, and O atoms are represented as blue, yellow, and red spheres, respectively.

the size of the system (for instance, we used a $4 \times 4 \times 1$ k-point mesh for a 24 C atom graphene supercell and $1 \times 1 \times 9$ for a 40 C atom (10,0) nanotube) were employed in order to guarantee convergence of the total energy per particle to within 0.5 meV/molecule. Typical system sizes ranged $6 \leq N \leq 32$ C atoms in graphene and $24 \leq N \leq 120$ C atoms in carbon nanotubes, depending on the doping concentration and CNT radius/chirality. All the structures considered were relaxed with a conjugate-gradient algorithm until the forces on the atoms were less than 0.01 eV/Å. To understand the electronic structure mechanisms underlying calcium-mediated carbon capture, we performed charge-density distribution (CDD) analysis on some of the optimized structures using the Bader theory.[30,31] Reported binding energies E_{bind} correspond to the energy difference between the geometry optimized total system and individually relaxed molecule and Ca-doped nanostructure monomers. Periodic boundary conditions were applied in all three dimensions and a vacuum of 30 Å was set so as to avoid spurious interactions between images.

III. RESULTS AND DISCUSSION

Very recently, we have predicted the existence of an equilibrium $(\sqrt{3} \times \sqrt{3})$ $R30°$ commensurate Ca monolayer adsorbed on graphene (e.g., CaC_6) that remains stable without clustering at low and room temperatures.[23] For carbon nanotubes, we also have demonstrated that uniformly Ca-decorated zigzag ($n \leq 10$,0) CNTs become stable against clustering at moderately large doping concentrations (~25−30%), whereas Ca-coated armchair (n, n) CNT exhibits a thermodynamic tendency for Ca aggregation (see Figure 1). In the following, we present results for the CCS behavior of the thermodynamically stable Ca-decorated nanostructures obtained in ref 23. In Table I, we summarize the corresponding binding energies per gas molecule and gas-uptake capacities as computed with DFT; those quantities are expressed as function of Ca concentration X_{Ca} which is defined as the ratio between the number of Ca and C atoms. Results enclosed in Table I must be considered as valid in the $P \rightarrow 0$ limit since the concentration of gas molecules considered in our simulations is very dilute (e.g., lower than 2×10^{-3} g CO_2/cm^3).

For pristine nanostructures (Figure 2), we found that CO_2 molecules bind very weakly to the carbon surfaces (physisorption) and prefer to accommodate on top of subjacent C−C bonds (graphene, d(mol − Gr) = 3.65 Å) or the center of carbon hexagons (CNTs, d(mol − CNT) = 3.52 Å). In contrast, the interactions of gas molecules with Ca-decorated nanostructures are generally much stronger. In the case of CNTs, the estimated binding energies per molecule are very large, of the order of an electronvolt, and tend to increase with Ca coverage. Corresponding CO_2-uptake capacities are also remarkably large, about a factor of 2−4 larger than the threshold value of 0.132 g CO_2/g sorbent. Concerning structural aspects, CO_2 molecules, which in the gas-phase or when physisorbed on pure carbon surfaces remain linear (θ(O−C−O) = 180° and d(C−O) = 1.18 Å), undergo large bending and C−O bond elongation (θ(O−C−O) = 62° and d(C−O) = 1.28 Å) as a consequence of significant electronic charge donation from the metal centers (~1 e^-). These results, together with visual inspection of the geometry optimized structures (Figure 2), indicate covalent CO_2 binding to the Ca−CNT surfaces. In Figure 3, we plot the dependence of CO_2 binding on the radius of zigzag CNT as obtained at low Ca-doping concentrations. We found that CO_2 binding increases almost linearly with decreasing CNT radius up to a limiting value of ~4 Å, corresponding to the (10,0) case. For smaller CNT radii, the molecular binding decreases by about 40%. We note that the $|E_{bind}|$ maximum observed in Figure 3 corresponds to the limiting radius reported in ref 23. for stable and uniform Ca decoration of CNTs, so that the strength of the CO_2 binding appears to be directly correlated with the strength of the Ca-CNT interactions.

For Ca-decorated graphene, intense molecular binding accompanied by large electronic charge transfers is also predicted at low doping concentrations. However, an abrupt change in the strength and nature of the gas-nanostructure interactions occurs at a coverage of 16.67% where gas molecules physisorb on the carbon surface (see Table I and Figure 2). This molecular binding transition is provoked by steric effects and may be of applicability in carbon capture since operating $P-T$ conditions depend critically on the nature of the gas-sorbent interactions. Specifically, densely doped graphene appears to be well-suited for low-T/low-P CCS application (e.g., fossil fuel postcombustion and ambient air conditions), whereas sparsely doped graphene shows promise for high-T/high-P carbon cycling (e.g., fossil fuel precombustion conditions).

To understand the electronic structure effects underlying Ca-mediated carbon capture process, we examined the partial density of electronic states (pDOS) corresponding to one CO_2 molecule interacting with a Ca adatom in graphene (Figure 4). We observed

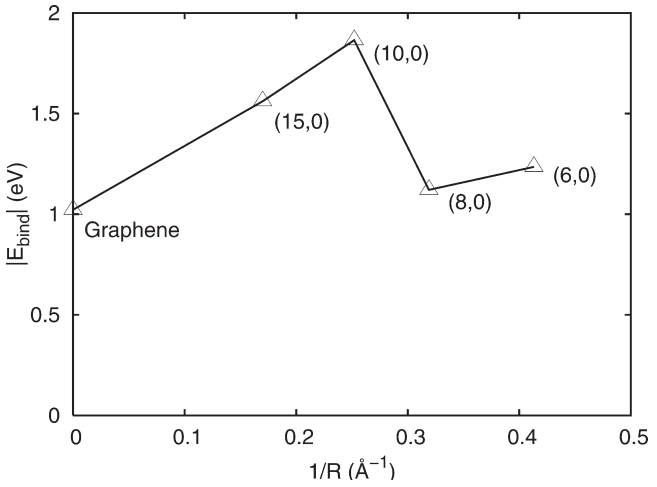

Figure 3. CO_2 binding energy as a function of the inverse of zigzag CNT radius for doping concentrations $0.0 < X_{Ca} \leq 5.0\%$. The solid line is a guide to the eye.

that the presence of Ca dopants induces important overlapping between clouds of electronic p molecular and s,d metallic states in the region near the Fermi level. Such a strong electronic orbital hybridization of dsp type is the main component for the enhancement of CO_2 binding to the carbon surfaces. According to CDD analysis, when Ca impurities adsorb on graphene these transfer a charge of about 0.8 e^- to the neighboring C atoms; in the presence of the CO_2 molecule, the metal cations become further positively charged by donating about 1.0 e^- to the neutral molecule. These electronic charge transfers are correlated with significant structural and electronic density rearrengements within the gas molecules. In particular, when the linear CO_2 bends the corresponding degenerate $1\pi_g$ highest-occupied molecular orbital (HOMO) bonding and $2\pi_u$ lowest-unoccupied molecular orbital (LUMO) antibonding orbitals split in two;[32] the resulting LUMO orbital has both σ and π character so that the molecule interacts more effectively with the s and d orbitals localized in the metal centers and electronic charge is transferred to the oxygen atoms. Electronic CCS mechanisms similar to the ones already described can be expected to occur also in other heavy alkali earth-metal doped carbon materials.

In predicting materials for practical gas capture/storage applications, an important aspect that has to be addressed is possible decomposition of the gas-loaded material into related substances.[33,34] We analyzed the stability of CO_2-loaded Ca-graphene/CNT systems against decomposition into calcium oxide, carbon monoxide, and graphene/CNT, by computing the energy difference

$$\Delta E = [E(\mathrm{CaO}) + E(\mathrm{CO}) + E(\mathrm{CNS})] - E(\mathrm{CO_2@Ca@CNS}) \quad (1)$$

where CNS represents for pristine graphene/CNT, E(CaO) is the energy of the equilibrium bulk CaO crystal and E(CO) represents the energy of one isolated CO gas molecule. Predicted ΔE values are −1.990 eV/molecule for graphene and −0.292 and −0.376 eV/molecule for (10,0) and (6,0) CNTs, respectively. This shows that the CO_2-loaded nanostructures are strongly (graphene) or moderately (CNTs) unstable against the formation of CaO and CO gas. At first glance, this conclusion might seem pessimistic since these sorbent regenerability issues are likely to be encountered in CCS cycling. However, there is a series of effects that derive from such a thermodynamic instability which could largely

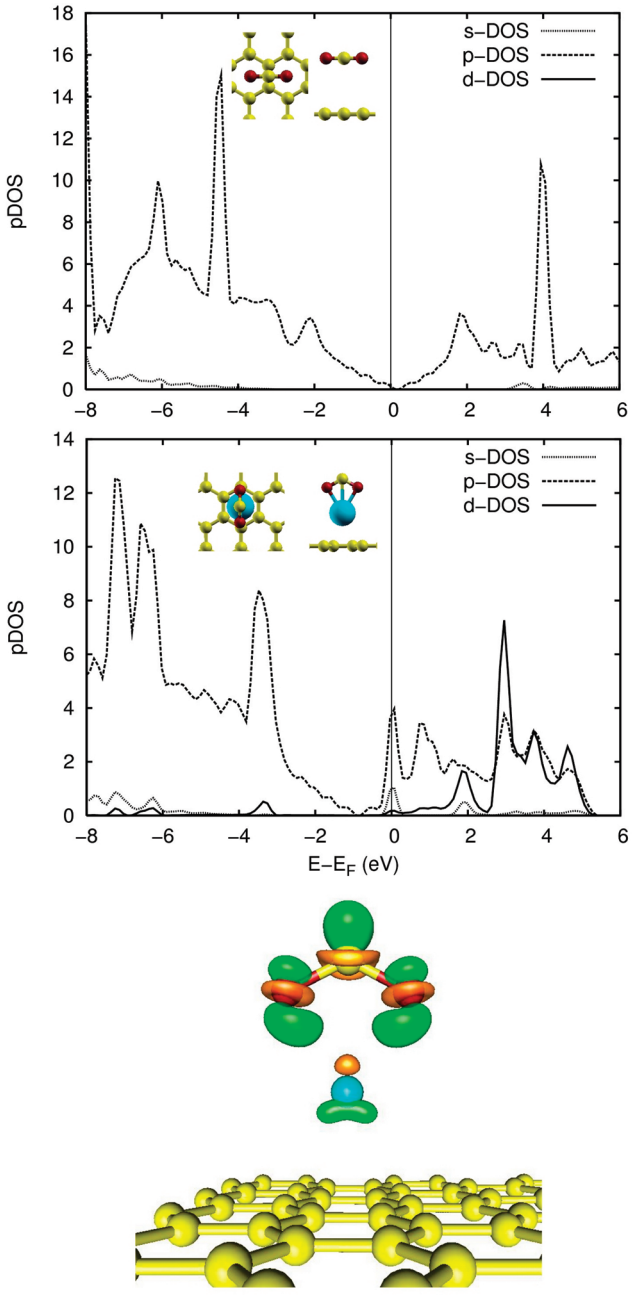

Figure 4. Partial density of electronic states corresponding to one CO_2 molecule adsorbed on pure graphene (a) and top of a Ca adatom (b). Orbital energies are expressed relative to the Fermi level E_F. (c) Deformation charge density plot corresponding to one gas molecule adsorbed on Ca-doped graphene; areas of electronic density accumulation (depletion) relative to the nondoped case are colored in green (orange).

compensate for recycling penalties, namely, (i) CO_2 is regenerated in situ into CO gas (so that some of the energy-consuming post-CCS transportation and regeneration processes could be saved) and (ii) nucleation of CaO clusters in the carbon surfaces will lead to further CCS enhancement via spontaneous formation of calcite[35] (e.g., $CaO + CO_2 \rightarrow CaCO_3$, with an enthalpy balance of $\Delta H = -1.636$ eV/molecule according to our calculations), thus final CO_2-uptake capacities may be about a factor of 2 larger than the values reported in Table I. Regarding (ii), it is worth

mentioning that CaO-based materials have already been proposed as efficient carbon sorbents[6] and that studies on the kinetics of reactions $Ca + CO_2 \rightarrow CaO + CO$ and $CaO + CO_2 \rightarrow CaCO_3$ at ambient conditions already exist in the literature.[36,37] Thermodynamic destabilization of materials for *in situ* CO_2 regeneration and enhanced CCS is an interesting new concept that appears to show potential for applications.

In view of the predicted large CO_2-uptake capacities of Ca-decorated nanostructures, it is important to check the relative adsorption strength of other molecules on these materials. Nitrogen is abundant in ambient air and also in flue gases, so we chose it as the most relevant molecule for comparison purposes. In pristine nanostructures, we found that CO_2 and N_2 molecules behave very similarly, that is, both physisorb. At low Ca-doping concentrations, however, the situation changes drastically, and N_2 molecules bind to the nanostructures much more weakly than CO_2 molecules (for instance, in (6,0) and (10,0) CNTs we obtained $|E_{bind}|$ values for N_2 that are about 40 and 60% smaller than those obtained for CO_2). Moreover, the interactions of N_2 molecules with Ca-decorated nanostructures do not appear to increase with increasing doping concentration, in contrast to what is observed for CO_2 (for example, N_2 E_{bind} = −0.645 eV/molecule and CO_2 E_{bind} = −2.731 eV/molecule in X_{Ca} = 12.5% graphene). Reassuringly, frontier molecular orbital calculations performed on a metal-doped (6,0) CNT and CO_2/N_2 molecule systems show that the energy difference between the HOMO of the nanotube and LUMO of the molecule amounts to 0.11 eV in CO_2 and 0.87 eV in N_2; thus higher CO_2-nanostructure reactivity is evidenced. These results lead to the conclusion that Ca-decorated nanostructures exhibit suitable CO_2/N_2 selectivity properties for CCS application.

IV. CONCLUSIONS

By use of first-principles simulation techniques we have predicted large CO_2-uptake capacities, decomposition-mediated CCS enhancement effect, and convenient CO_2/N_2 selectivity properties for Ca-decorated carbon nanostructures. In the case of graphene, we also find that the strength of the CO_2-dopant interactions can be efficiently tuned via variation of the metal doping concentration. Enhancement of the CO_2 reactivity properties of carbons in the presence of calcium adatoms can be understood in terms of electronic structure, namely, overlapping of s,d-metallic and p-molecular states in the region near the Fermi level and splitting of LUMO $2\pi_u$ molecular orbitals induced by bending. The Ca-mediated CCS enhancement effect found in this work can be expected to also occur for other carbon materials such as activated carbons, graphite, and nanohorns, which are cheaper to produce than nanostructures. In view of the present great demand on materials for CO_2 capture, we encourage experimental searches to synthesize and gauge the potential of these promising C/Ca-based materials.

AUTHOR INFORMATION

Corresponding Author
*E-mail: z.x.guo@ucl.ac.uk.

ACKNOWLEDGMENT

The authors acknowledge support by the EPSRC SUPERGEN Initiative under UK-SHEC (GR/S26965/01, EP/E040071/1), STEPCAP (EP/G061785/1), and Platform Grant (GR/S52636/01, EP/E046193/1).

REFERENCES

(1) Metz, B; Davidson, O.; de Coninck, H.; Loos, M.; Meyer, L. *Intergovernmental Panel on Climate Change (IPCC). Special Report on Carbon Dioxide Capture and Storage*; Cambridge University Press, Cambridge, 2005.
(2) Jones, N. *Nature* **2009**, *458*, 1094.
(3) Keith, D. W. *Science* **2009**, *325*, 1654.
(4) Zeman, F. *Environ. Sci. Technol.* **2007**, *41*, 7558.
(5) Aaron, D.; Tsouris, C. *Sep. Sci. Technol.* **2005**, *40*, 321.
(6) Choi, S.; Drese, J. H.; Jones, C. W. *ChemSusChem* **2009**, *2*, 796.
(7) Drage, T. C.; Blackman, J. M.; Pevida, C.; Snape, C. E. *Energy Fuels* **2009**, *23*, 2790.
(8) Cazorla-Amorós, D.; Alcañiz-Monges, J.; Linares-Solano, A. *Langmuir* **1996**, *12*, 2820.
(9) Martín, C. F.; Plaza, M. G.; Pis, J. J.; Rubiera, F.; Pevida, C.; Centeno, T. A. *Sep. Purif. Technol.* **2010**, *74*, 225.
(10) Mazumber, S.; van Hemert, P.; Busch, A.; Wolf, K-H. W. W.; Tejera-Cuesta, P. *Int. J. Coal Geol.* **2006**, *67*, 267.
(11) Maroto-Valer, M. M.; Tang, Z.; Zhang, Y. *Fuel Process. Technol.* **2005**, *86*, 1487.
(12) Plaza, M. G.; Pevida, C.; Arenillas, A.; Rubiera, F.; Pis, J. J. *Fuel* **2007**, *86*, 2204.
(13) Plaza, M. G.; Pevida, C.; Arias, B.; Casal, M. D.; Martín, C. F.; Fermoso, J.; Rubiera, F.; Pis, J. J. *J. Environ. Eng.: ASCE* **2009**, *135*, 426.
(14) Pevida, C.; Drage, T. C.; Snape, C. E. *Carbon* **2008**, *46*, 1464.
(15) Pevida, C.; Plaza, M. G.; Arias, B.; Fermoso, J.; Rubiera, F.; Pis, J. J. *Appl. Surf. Sci.* **2008**, *254*, 7165.
(16) Agnihotri, S.; Rood, M. J.; Rostam-Abadi, M. *Carbon* **2005**, *43*, 2379.
(17) Bienfait, M; Zeppenfeld, P.; Dupont-Pavlovsky, N.; Muris, M.; Johnson, M. R.; Wilson, T.; DePies, M.; Vilches, O. E. *Phys. Rev. B* **2004**, *70*, 035410.
(18) Zhao, J.; Buldum, A.; Han, J.; Lu, J. P. *Nanotechnology* **2002**, *13*, 195.
(19) Cinke, M.; Li, J.; Bauschlicher, C. W., Jr.; Ricca, A.; Meyyappan, M. *Chem. Phys. Lett.* **2003**, *376*, 761.
(20) Du, A. J.; Sun, C. H.; Zhu, Z. H.; Lu, G. Q.; Rudolph, V.; Smith, S. C. *Nanotechnology* **2009**, *20*, 375701.
(21) Sun, Q.; Wang, Q.; Jena, P.; Kawazoe, Y. *J. Am. Chem. Soc.* **2005**, *127*, 14582.
(22) Li, S.; Jena, P. *Phys. Rev. Lett.* **2006**, *97*, 209601.
(23) Cazorla, C.; Shevlin, S. A.; Guo, Z. X. *Phys. Rev. B* **2010**, *82*, 155454.
(24) Irons, R.; Goh, B.; Snape, C. E.; Arenillas, A.; Drage, T.; Smith, K.; Maier, J.; Dhungel, B.; Jackson, P.; Sakellaropoulos, G.; Stathopoulos, V.; Skodras, G. *Assessment of options for CO_2 capture and geological sequestration. Comparison of CO_2 capture technologies and enhancing CMM production with CO_2*, European Comission, ISBN-9789279115905 2007.
(25) Blöchl, P. E. *Phys. Rev. B* **1994**, *50*, 17953.
(26) Perdew, J. P.; Burke, K.; Ernzerhof, M. *Phys. Rev. Lett.* **1996**, *77*, 3865.
(27) Kresse, G.; Furthmüller, J. *Phys. Rev. B* **1996**, *54*, 11169.
(28) Sun, Y. Y.; Lee, K.; Wang, L.; Kim, Y.-H.; Chen, W.; Chen, Z.; Zhang, S. B. *Phys. Rev. B* **2010**, *82*, 073401.
(29) Cazorla, C. *Thin Solid Films* **2010**, *518*, 6951.
(30) Bader, R. G. W. *Atoms in Molecules. A Quantum Theory*; Oxford University Press: New York, 1990.
(31) Henkelman, G.; Arnaldsson, A.; Johnsson, H. *Comput. Mater. Sci.* **2006**, *36*, 354.
(32) Wang, S.-G.; Liao, X.-Y.; Cao, D.-B.; Huo, C.-F.; Li, Y.-W.; Wang, J.; Jiao, H. *J. Phys. Chem. C* **2007**, *111*, 16934.
(33) Cobian, M.; Íñiguez, J. *J. Phys.: Condens. Matter* **2008**, *2*, 285212.

(34) Srinivas, G.; Howard, C. A.; Bennington, S. M.; Skipper, N. T.; Ellerby, M. *J. Mater. Chem.* **2009**, *19*, 5239.
(35) Pacchioni, G.; Ricart, J. M.; Illas, F. *J. Am. Chem. Soc.* **1994**, *116*, 10152.
(36) Broadley, S.; Vondrak, T.; Wright, T. G.; Plane, J. M. C. *Phys. Chem. Chem. Phys.* **2008**, *10*, 5287.
(37) Plane, J. M. C.; Rollason, R. J. *J. Phys. Chem. A* **2001**, *105*, 7047.